Environmental Fluid Mechanics (2005) 5: 87–107

Mercury Budget Estimates for the State of New York

A. VOUDOURI, I. PYTHAROULIS and G. KALLOS*
University of Athens, Division of Applied Physics, Panepistimioupolis Bldg Phys V, Athens, Greece

Received 10 July 2003; accepted in revised form 13 February 2004

Abstract. The development of two comprehensive modelling systems and a test application to estimate the mercury budget for the State of New York is discussed in the present study. The modelling tools developed are based on two well known meteorological modelling systems namely, RAMS and SKIRON/Eta. Both models have been modified and the developed modules describing the physicochemical processes of mercury have been incorporated in each modelling system. Model calculations and measurements have been compared during the 14 to 26 August 1997 simulation period. Two different simulations were performed, 'scenario1' where all available sources of mercury were used and 'scenario2' where the New York State mercury sources were excluded. An attempt was made to identify and quantify critical gaps in the current understanding of regional scale transport deposition and fate of mercury in New York State, improving modelling capabilities and understanding of mercury as an air pollutant, and provide a tool for policy makers in mitigating the impacts of mercury pollution.

Key words: deposition, gaseous, model intercomparison, particulate mercury, transformation, transport

1. Introduction

Mercury is a highly toxic pollutant emitted to the atmosphere from different natural and anthropogenic sources. Main sources of mercury due to human activity include power plants (burning coal and oil), chemical plants (e.g., chlor-alkali plants), waste incinerators, ferrous foundries, non-ferrous metal smelters, refineries, and cement kilns. Additional contributions of mercury come from natural sources such as the earth mantle and volcanoes. There are many difficulties encountered when trying to measure the mercury concentration therefore over the past years several studies have been conducted using mathematical models to describe the behaviour of mercury released into the atmosphere.

This study is focused on two major model developments for studying the transport, transformation and deposition of mercury in New York State. The developed

*Corresponding author, E-mail: kallos@mg.uoa.gr

modules for the physico-chemical processes of mercury have been incorporated in two well-known atmospheric models: the Regional Atmospheric Modelling System (RAMS; [1, 2]) and the SKIRON/Eta [3, 4]. In each model, basic processes like advection and diffusion are the ones already existing for passive tracers that were modified accordingly. The modules for the various atmospheric and surface processes of mercury species deal with the preparation of emissions from anthropogenic and natural sources, the chemical and physical transformations of mercury in the atmosphere with changing meteorological conditions, dry deposition over water surface and over land as well as the wet removal process concerning the soluble chemical species (Hg^2 and its compounds, and some Hg^0), and also particulate matter scavenged from below the precipitating clouds. The use of two atmospheric models allowed the inter-comparison of the results and, therefore improved understanding on the mercury modelling. The inter-comparison of the results is a necessary process for avoiding systematic errors since there are no systematic measurements available for the mercury species in several locations for performing other inter-comparison studies.

Two different simulations were performed during August 1997 (14/8 to 26/8) for the State of New York. For the first simulation 'scenario1' all available sources of mercury were used, while for the second simulation 'scenario2' the New York State mercury sources were extracted. The specific scenarios were selected in an attempt to investigate the contribution of mercury sources located in the State of New York to the local depositions of mercury. The general purpose of this work was to study whether the reduction of mercury emissions at regional scale can affect the amounts of deposited mercury within a specific area. This is a rather ambitious purpose as mercury is characterised as a multi-scale pollutant [27] able to be transported and deposited at local, regional and global scales.

2. Model Description and Set-Up

The transport, transformation and deposition of mercury in New York State have been investigated using the RAMS and SKIRON/Eta modelling systems. Both models have been modified and the developed modules describing the various atmospheric and surface processes of mercury species are briefly described below:
a. Emissions processor: This module deals with the preparation of emissions from anthropogenic and natural sources. It utilises the data stored in the Mercury Emission Inventory (MEI). The various sources (power plants, waste incinerators, cement kilns, chlor-alkali production) are allocated within the model domain (point sources). The module defines emissions according to the land use (area sources), initial and lateral boundary conditions according to the type of simulation; initial run (coldstart) or continuation run (hotstart). The entire module is very flexible because the MEI should be updated easily and the source allocation is automatic according to the geographic co-ordinates and the type of sources. Stack character-

istics can be added easily in case they are available, and sources are attributed to the appropriate model level.

Re-emission involves gaseous evasion of previously deposited mercury in water and soil and is also considered in both models. Fluxes of mercury from soil and water are taken into account.

A parameterization of the mercury fluxes from the sea is included in the mercury emissions processor. The fluxes are approximated by a hyperbolic tangent empirical function that mainly depends on air/water temperature difference and the wind speed at 10m height. This function was formulated in such a way so that the fluxes of mercury from the sea lie within the range reported or inferred by the literature, [5–7]. In the literature, the average observed concentrations of Hg^0 in lakes and oceans range significantly from about 20 ng/m^3 to 2000 ng/m^3 [8–9]. In general, there is a large uncertainty about the spatial and temporal variations of elemental mercury concentration in surface water. Also, the work of Xu *et al.* [7] indicated that it is unclear how important are the emissions from the water bodies (lakes and oceans) relative to the anthropogenic or plant emissions. A detailed parameterization of air-water exchange of mercury may be required in case the emissions from water bodies appear to be important for the mercury concentrations.

b. Chemistry module: The chemistry module deals with the gas and aqueous phase chemistry reactions of mercury species with other reactants. The gas phase chemistry reactions of mercury considered in this chemistry module are those with ozone and hydrogen peroxide. Elemental Hg is also believed to react with other radical species [10]; however these reactions of gaseous mercury have not been treated at the present version of the model.

The aqueous phase chemistry is much more complex than that of the gas phase. There are a number of oxidation reactions which may occur, a number of these involve photolytically produced radicals, resulting in different day and night-time oxidation rates. Oxidation by dissolved ozone is many times faster than the corresponding gas phase reaction, and there is competition from OH, HOCl and OCl^- radicals. In the present module, these last three species are produced in the gas phase and then partitioning between the gas and aqueous phase is considered [11]. Their production is governed by photolytic processes and partitioning by the radius of the droplets present and the liquid water content of the atmosphere. It should be noted that HOCl and OCl^- are also produced in the aqueous phase by dissolution of molecular chlorine gas [12]. There is a range of possible complexation products of more or less importance depending on the pH of the aqueous phase and on the chemical composition of the original aerosol particle. For instance in fog and cloud droplets the major complexing agent is the OH^- ion, as it is for sulphate/nitrate aerosol particles. In sea-salt aerosol Cl^- and Br^- ions play the most important role [11].

The full database of mercury chemical reactions contains over 400 gas phase, aqueous phase, heterogeneous and photolytic reactions, as well as gas-aqueous mass transfer equilibrium. However this chemistry module handled those reactions

that mainly contributed to the production/loss of the pollutant. The full list of mercury reactions, originally adapted at the framework of MAMCS project (MAMCS, 2000) that was also used in the present study is summarized in Table 1.

One of the benefits of the chemistry module incorporated in RAMS and SKIRON/Eta is its flexibility, and the simplicity with which new reactions may be added to the database.

c. Dry deposition module: In most deposition models one determines the deposition velocity, v, of a pollutant associated with particulate matter of a given radius and density, over a given surface [38]. The pollutant flux F (pg/m^{2}s) is defined by the relation,

$$F = C\,v, \tag{1}$$

where C is the pollutant concentration, which is assumed constant in the deposition layer. In the dry deposition process the velocity is calculated using the resistance method. Using this method deposition is calculated as the sum of various resistances [17], and the settling velocity for particles:

$$\mathrm{v} = [\mathrm{R_a} + \mathrm{R_b} + \mathrm{R_a R_b V_g}]^{-1} + \mathrm{V_g}, \tag{2}$$

where the subscripts for the resistances R, represent the atmospheric layers, a is the quasi-laminar sub-layer, b is the bulk resistance of various surfaces, and $\mathrm{V}_g$is the gravitational settling velocity. The values of the resistances depend upon meteorological conditions as well as on the properties of the surface.

The model proposed by Williams [13] and modified later by Pirrone *et al.* [14, 15] for trace metals and semi-volatile organic pollutants is used to calculate the deposition fluxes over water surfaces, whilst Slinn and Slinn's model [16] is used for deposition over soil and vegetation. These modules consider super micron particle eddy diffusivity, gravitational settling and particle inertia as the main mechanisms influencing the deposition to terrestrial receptors. In order to reduce the uncertainty associated with the deposition fluxes of atmospheric mercury to terrestrial receptors the suggestions of Hicks *et al.* [17] have been adopted.

As already stated the gaseous flux of Hg^0 from air to land/water surface is assumed to be zero [18]. However a non-negligible flux of gaseous $Hg^0$is taken into account by the gas-particle module described in details in Pirrone *et al.* [18]. In fact, due to the diffusion of Hg^0 to the particulates, a small fraction of Hg^0 remains trapped in and then deposited with the aerosol particle. This process, which so far has been neglected in other models, has been examined at the present study, through expensive sensitivity experiments in an attempt to investigate the contribution of Hg^0 adsorbed in Total Suspended Particles (TSPs) to total deposition. The calculated deposited amounts (wet and dry) of Hg^0 adsorbed were found to fall within the range of model uncertainties therefore are not considered at the discussion.

The deposition velocity of Hg associated with particles (Hg^p) was calculated by distributing its mass according to a lognormal particle size distribution. The whole

Table I. The Hg chemical reactions considered in the chemistry module.

Mercury reactions and equilibria	k or K	Reference
$Hg^0_{(aq)} + O_{3(aq)} \rightarrow HgO_{(aq)}$	$4.7\ 10^7\ M^{-1}\ s^{-1}$	[34]
$HgO_{(aq)} + H^+_{(aq)} \rightarrow Hg^{++}_{(aq)} + OH^-_{(aq)}$	$1\ 10^{10} M^{-1}\ s^{-1}$	[36]
$Hg^{++}_{(aq)} + OH^-_{(aq)} \leftrightarrow HgOH^+_{(aq)}$	$3.9\ 10^{10}\ M^{-1}$	[36]
$HgOH^+_{(aq)} + OH^-_{(aq)} \leftrightarrow Hg(OH)_{2(aq)}$	$1.6\ 10^{11}\ M^{-1}$	[36]
$HgOH^+_{(aq)} + Cl^-_{(aq)} \leftrightarrow HgOHCl_{(aq)}$	$2.7\ 10^7\ M^{-1}$	[36]
$Hg^{++}_{(aq)} + Cl^-_{(aq)} \leftrightarrow HgCl^+_{(aq)}$	$5.8\ 10^6\ M^{-1}$	[36]
$HgCl^+_{(aq)} + Cl^-_{(aq)} \leftrightarrow HgCl_{2(aq)}$	$2.5\ 10^6\ M^{-1}$	[36]
$HgCl_{2(aq)} + Cl^-_{(aq)} \rightarrow HgCl^-_{3(aq)}$	$6.7\ M^{-1}$	[29]
$HgCl^-_{3(aq)} + Cl^-_{(aq)} \rightarrow HgCl^-_{4(aq)}$	$13\ M^{-1}$	[29]
$Hg^{++}_{(aq)} + Br^-_{(aq)} \rightarrow HgBr^+_{(aq)}$	$1.1\ 10^9\ M^{-1}$	[29]
$HgBr^+_{(aq)} + Br^-_{(aq)} \rightarrow HgBr_{2(aq)}$	$2.5\ 10^8\ M^{-1}$	[29]
$HgBr_{2(aq)} + Br^-_{(aq)} \rightarrow HgBr^-_{3(aq)}$	$1.5\ 10^2\ M^{-1}$	[29]
$HgBr^-_{3(aq)} + Br^-_{(aq)} \rightarrow HgBr^-_{4(aq)}$	$23\ M^{-1}$	[29]
$Hg^{++}_{(aq)} + SO^-_{3(aq)} \leftrightarrow HgSO_{3(aq)}$	$5\ 10^{12}\ M^{-1}$	[36]
$HgSO_{3(aq)} + SO^-_{3(aq)} \leftrightarrow Hg(SO_3)^-_{2(aq)}$	$2.5\ 10^{11}\ M^{-1}$	[36]
$HgSO_{3(aq)} \rightarrow Hg^0_{(aq)} +$ products	$0.6\ s^{-1}$	[33]
$Hg^0_{(aq)} + OH_{(aq)} \rightarrow Hg^+_{(aq)} + OH^-_{(aq)}$	$2.0\ 10^9\ M^{-1}\ s^{-1}$	[30]
$Hg^+_{(aq)} + OH_{(aq)} \rightarrow Hg^{++}_{(aq)} + OH^-_{(aq)}$	$1.0\ 10^{10}\ M^{-1}\ s^{-1}$	[30]
$Hg^{II}_{(aq)} + O^-_{2(aq)} \rightarrow Hg^+_{(aq)} + O_{2(aq)}$	$1.1\ 10^4\ M^{-1}\ s^{-1}$	[35]
$Hg^{II}_{(aq)} + HO_{2(aq)} \rightarrow Hg^+_{(aq)} + O_{2(aq)} + H^+_{(aq)}$	$1.1\ 10^4\ M^{-1}\ s^{-1}$	[35]
$Hg^+_{(aq)} + O^-_{2(aq)} \rightarrow Hg_{(aq)} + O_{2(aq)}$	fast	[35]
$Hg^+_{(aq)} + HO_{2(aq)} \rightarrow Hg^0_{(aq)} + O_{2(aq)} + H^+_{(aq)}$	fast	[35]
$Hg_{(aq)} + HOCl_{(aq)} \rightarrow Hg^{++}_{(aq)} + Cl^-_{(aq)} + OH^-_{(aq)}$	$2.09\ 10^6\ M^{-1}\ s^{-1}$	[35]
$Hg_{(aq)} + ClO^-_{(aq)} \rightarrow Hg^{++}_{(aq)} + Cl^-_{(aq)} + OH^-_{(aq)}$	$1.99\ 10^6\ M^{-1}\ s^{-1}$	[30]
$Hg^0_{(g)} \leftrightarrow Hg^0_{(aq)}$	$0.13\ M\ atm^{-1}$	[27]
$HgO_{(g)} \leftrightarrow HgO_{(aq)}$	$2.69\ 10^{12}\ M\ atm^{-1}$	[27]
$HgCl_{2(g)} \rightarrow HgCl_{2(aq)}$	$2.75\ 10^6\ M\ atm^{-1}$	[27]
$HgO_{(g)} \rightarrow$ deposition	$2.0\ cm\ s^{-1}$	[11]
$HgCl_{2(g)} \rightarrow$ deposition	$2.0\ cm\ s^{-1}$	[11]

particle size distribution is subdivided into 15 size intervals and the deposition velocity is calculated for each. The calculated deposition velocity depends on the wind speed, air/water temperature difference (over water surfaces) and particle size [13]. Thus the deposition velocity of Hg^p is obtained as a weighted average of the previous velocities.

d. Wet deposition module: The wet removal process concerns the soluble chemical species (Hg^2 and its compounds, and some Hg^0) and also particulate matter scavenged from below the precipitating clouds.

This module calculates the amount of gaseous and particulate mercury scavenged from the atmosphere by precipitation events. The wet deposition is controlled by two contributory paths. The first derives from the continuous transfer of mercury to the cloud water as described by the chemistry module. There are two limiting factors here, the rate of uptake of gas phase elemental mercury, which is regulated by Henry's constant, and the subsequent oxidation of Hg^0 to Hg^2 which is governed by the reaction rate constants and the initial reactant concentrations. The deposition via this path depends upon the liquid water content of the cloud and the percentage of the droplets in the cloud, which reach the earth's surface.

The second path for the wet deposition of mercury is the physical removal of mercury particles in the presence of raining clouds. An assumption is made that mercury particles are then attached to the hydrometeors and fall to the ground. Thus the scavenging coefficient in both models is assumed to be generally unit, although this assumption may result to slightly overestimate the wet deposited values.

The wet deposition module has been validated and calibrated by using ad-hoc measurements performed at five sites in the Mediterranean Basin, and also by using long-term records of mercury in rainfall that have been collected in Europe during the last decade. The wet deposition module has been integrated into the overall model design in order to calculate the amount of mercury deposited by precipitation scavenging.

2.1. MODELS SETUP

2.1.1. *Atmospheric Models Set-Up*

The simulation performed with both models started at 0000 UTC on 14 August 1997 and ended at 0006 UTC 26 August 1997. The domain of both simulations (with and without the NY sources) covers the area of US East of the Rocky Mountains. The grid for RAMS has been selected with $90 \times 90 \times 30$ points and 36 km horizontal grid increment. The coordinates of the center of the domain were at 36.926° N and 85.037° W.

For the SKIRON/Eta model the selected area extends from 21.5° N to 48.8° N and from 63.8° W to 107.3° W, centered at 36.9° N and 85° W. This grid covers the same area with the one used for RAMS with minor differences attributed to the horizontal projection of each model.

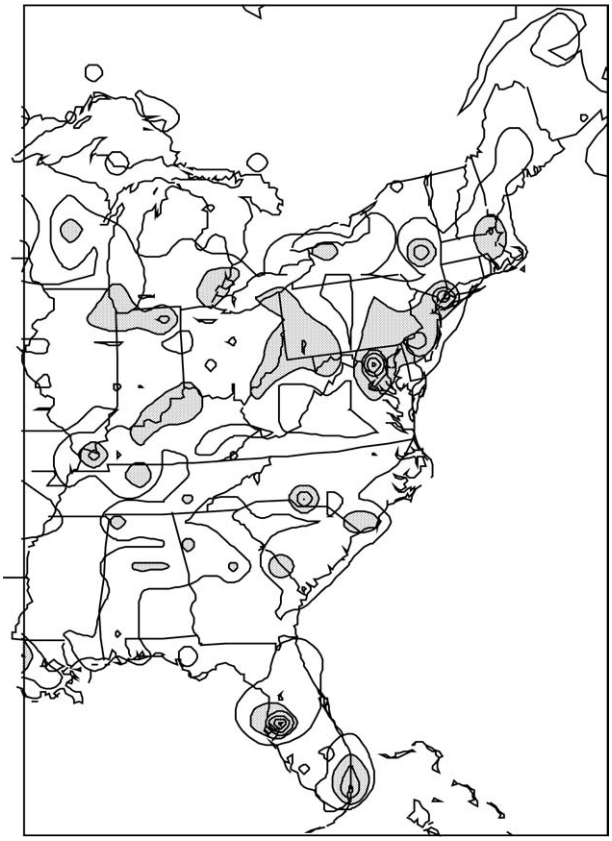

Figure 1. Spatial distribution of total gaseous and particulate emission rates in eastern North America. Emissions are summed over Lambert-conformal 80 × 80 km^2 areas, and contours are drawn at 90%, 70%, 50%, 30%, 10% and 1% of the maximum emission rate (west of Washington D.C.) of 23215 moles Hg per year per 80 × 80 km^2 area. Total emissions in domain = 5.26 × 10^5 moles year^{-1} (Source: Walcek *et al.*, 2003.)

2.1.2. *Mercury Modules Set-Up*

a. Emissions data: The New York State Department of Environmental Conservation provided the emission data used in both models. This mercury emission inventory includes all categories of sources (area, point sources). The emissions data contain information for each point source such as the location of the source, latitude and longitude, stack height, information on the emission type (Hg^0, Hg^2 and Hg^P) and type of plant. The final processing of this inventory was performed by Walcek *et al.* [19]. The spatial distribution of total gaseous and particulate emission rates in eastern North America is illustrated in Figure 1 for the first scenario. Mercury emissions extracted from the Global Mercury Emission Inventory have been also used for the rest computational domain. A second simulation was performed without using the New York State sources (second scenario).

b. Initial and boundary conditions for Hg^0, Hg^2 and Hg^P: Horizontally homogeneous initial and boundary conditions were used for the three mercury species. The boundary concentrations of all species were fixed throughout the simulations. Constant initial and lateral boundary concentrations of 1.4 ng/m^3, 80 pg/m^3 and 10 pg/m^3 were used for Hg^0, Hg^2 and Hg^P, respectively, in the lowest 2 km [20–22]. Shannon and Voldner (1995) have also estimated the background concentration of Hg^P to be equal to 10 pg/m^3 near the ground.

The initial and lateral boundary concentrations of the three species were assumed to decrease with height. Hg^0 decreases linearly with height above 2 km, reaching the 70% of its low-level concentration at 6 km. At this height, the background concentration of Hg^0 becomes equal to 0.92 ng/m^3. From 6 km to the model upper limit (18 km), the background concentration of Hg^0 decreases linearly to a negligible concentration.

The background concentration of Hg^2 and Hg^P decreases with height above 2 km, practically vanishing at the top of the model domain. More recent measurements of stratospheric aerosol particles showed that mercury can also be found at altitudes up to 19 km [24]. These concentrations were not considered at the present version of the model. However the concentrations at these heights are not expected to have significant effects on the results presented, as the majority of the removal processes occur within the lower half of the troposphere. Furthermore, in an attempt to minimize the uncertainties or influences of the initial conditions the first twenty-four hours of the simulation were not considered.

3. Results and Discussion

3.1. METEOROLOGICAL CONDITIONS

A detailed meteorology has been derived for the 14 to 26 August 1997 simulation period using RAMS and SKIRON/Eta system. Detailed meteorology is critical to improve the mercury concentration estimates, and to define the wet deposition patterns, as the total precipitation is determinative, especially for Hg^2 and Hg^P species.

Meteorological data, such as temperature, wind speed and direction, derived from RAMS model, indicated that a strong southerly flow was established over the northeastern US during the first day of simulation while near surface temperature over the northeastern US did not exceed 20 °C. On 21 August 1997, a deep low-pressure system extended over the State of New York inducing a strong north-easterly flow. Strong southerlies dominated over the Atlantic Ocean reaching the north-eastern coast of US. Strong north-westerlies were evident over the Canadian borders at the time. The increasing temperature and the strengthening of south-westerly flow are important parameters that influence the dispersion and diffusion of mercury over the New York State. These conditions can support the transfer of mercury from the eastern seaboard towards the New York State.

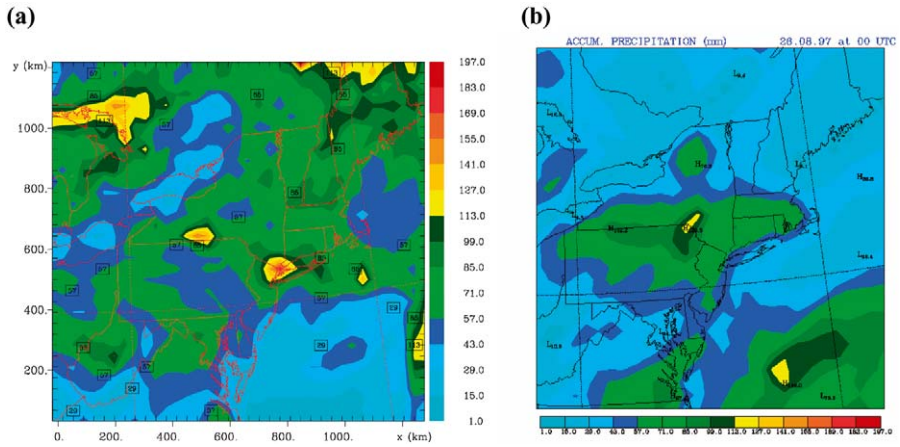

Figure 2. 12-days (14–26 August 1997) accumulated rain (mm), from (a) RAMS system (b) SKIRON/Eta system.

The calculated accumulated rain, within the 12 days of simulation is illustrated in Figures 2a, b (focused mainly on the State of New York) from RAMS and SKIRON/Eta systems respectively. It is evident that the total accumulated rain calculated from both models exhibits differences that can be attributed to the behaviour of the convective scheme used in each model (RAMS and SKIRON/Eta). SKIRON/Eta model uses the Betts-Miller-Janjic precipitation scheme, which tends to overestimate the precipitation areas without overestimating the precipitated water [25]. On the contrary, the RAMS microphysical scheme calculates higher amounts of precipitation in more restricted areas, leading to local peaks. These differences on the accumulated rain patterns can strongly influence the mercury wet deposition patterns.

3.2. SIMULATION PERFORMED WITH ALL SOURCES-SCENARIO 1

The concentration of mercury species is controlled by many factors that affect the chemical and physical processes such as atmospheric reactions and deposition. It also depends strongly on flow conditions and source locations [26]. In this study an attempt was made to investigate the relative contributions of in-state mercury sources and out-state sources to the mercury deposition in New York State. The first simulation performed with all available sources located over NE USA (scenario 1) showed that the Hg^0 concentrations, illustrated in Figure 3a, were lower than 1.6 ng/m^3 over the State of New York. However higher concentrations (more than 1.8 ng/m^3) were calculated near the sources and downwind of the State of New York following the north-easterly flow.

Hg^2 and Hg^P concentrations were still high around the sources for selected periods during the day (see Figures 3b, c). This can be attributed to the photochemical reactions producing Hg^2 and Hg^P during the daytime and to the poor dispersion

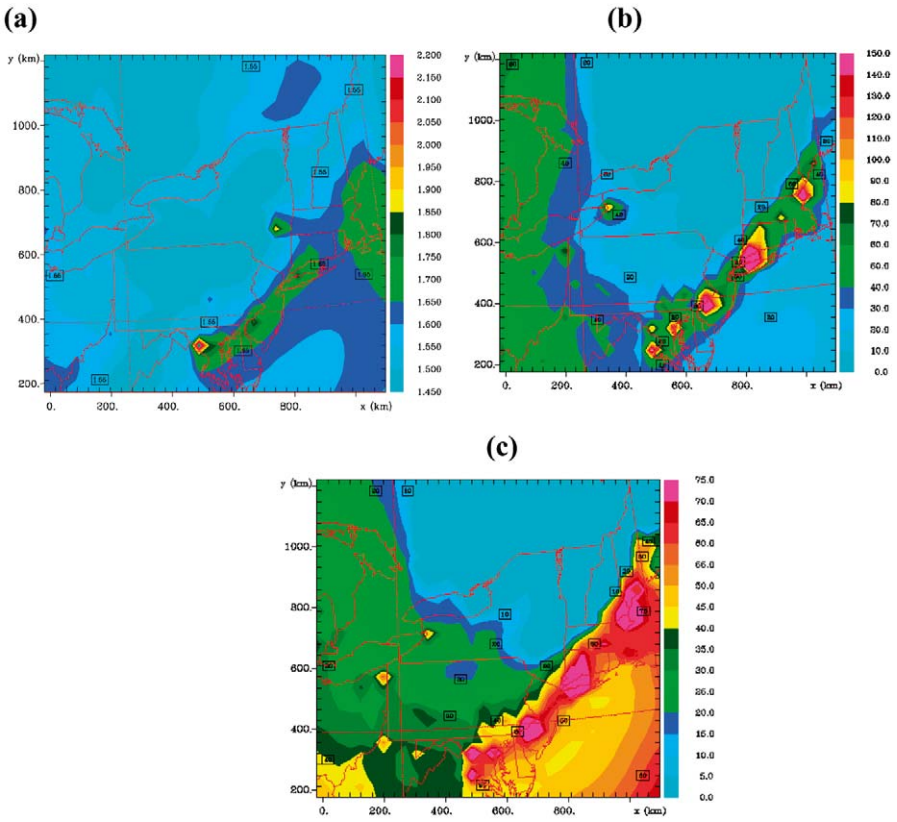

Figure 3. Mercury concentrations at the first model level (∼ 69 m) at 0000 UTC on 24 August 1997 from RAMS model of (a) Hg^0 (in ng/m^3), (b) Hg^2 (in pg/m^3) and (c) Hg^P (in pg/m^3).

conditions prevailing at the time. This is also consistent with the literature [27], as Hg^0 is known as a long-range transport pollutant, while Hg^2 can be removed in the vicinity of a few tens to a few hundreds of kilometres. In addition Hg^P species are likely to be deposited at intermediate distances depending on the prevailing wash-out mechanisms. These differences on the transport mechanisms for each species are clearly illustrated in the concentration patterns of Hg^0, Hg^2 and Hg^P presented in Figures 3a,b,c, respectively. It should be noted that all figures presented, illustrating mercury concentration and deposition are focused on a part of the computational domain that covers mainly the State of New York in an attempt to highlight differences exhibited over the area in both scenarios.

It is known that mercury enters the aquatic environment through the deposition processes. Therefore, it is important to estimate the amount of mercury species deposited through different atmospheric processes. Mechanisms used to describe the transport of Hg^0, Hg^2 and Hg^P and deposition of Hg^2 and Hg^P have been incorporated in both models. Therefore an attempt was made to calculate the accumulated deposition patterns for the simulation period. More specifically, the wet

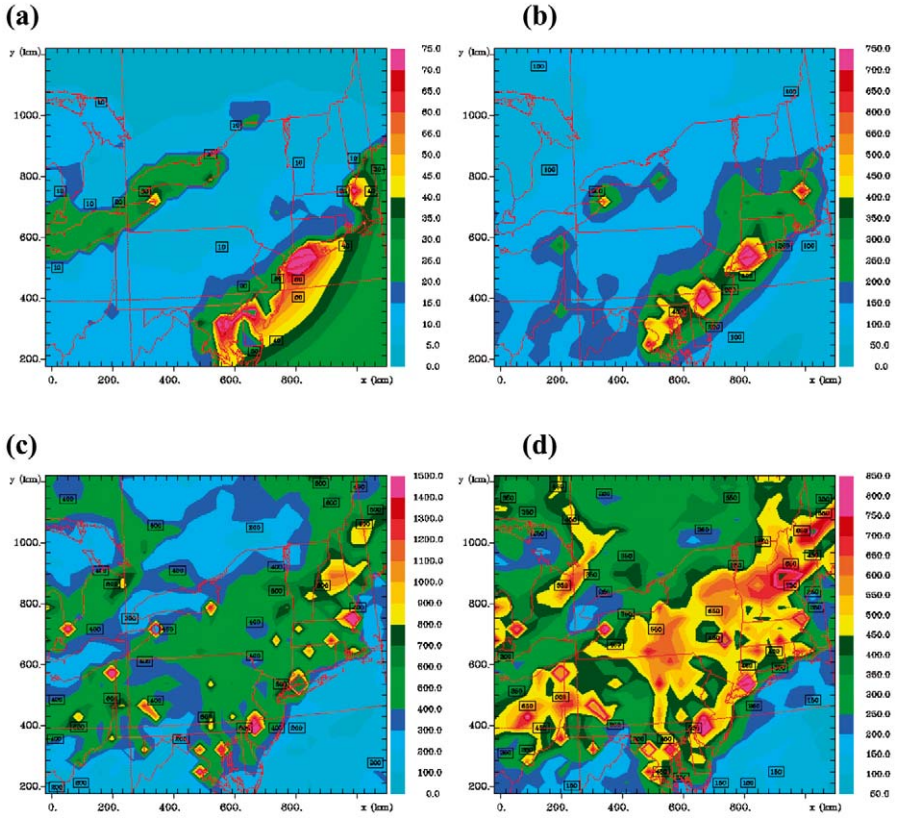

Figure 4. Dry and wet deposition at 0000 UTC on 24 August 1997 after 10 days of simulation, estimated from RAMS model. (a) Dry deposition of Hg^P (in ng/m^2), (b) Dry deposition of Hg^2 (in ng/m^2), (c) Wet deposition of Hg^2 (in ng/m^2) and (d) Wet deposition of Hg^p (in ng/m^2).

and dry deposition patterns of Hg^P and Hg^2 were estimated using both RAMS and SKIRON/Eta modelling systems.

The dry deposition patterns of mercury species are varying over sea and over land. The transport of mercury species is dependent upon the advective transport by the mean wind and transport by turbulent dispersion. The spatial and temporal variations on the dry deposition patterns can be determined through the similarities with the conventional pollutants. The accumulated (during 10 days of the simulation) amounts of Hg^P that is deposited through dry processes in the simulation are greater over the sea than over land as illustrated in Figure 4a. The dry deposition pattern of Hg^P depends on the pollutant concentration and the deposition velocity. The deposition velocity of Hg^P used in these simulations is a weighted average of 15 deposition velocities, corresponding to the 15 size intervals at which particles are distributed. Over regions with high humidity (e.g., over sea surface) greater deposition velocities are observed due to the dependence of the deposition velocity on the size of the particles. Particles sizes under these conditions are relatively high.

Dry deposition pattern of Hg^2 is illustrated in Figure 4b. The highest amounts of the pollutant are deposited near the sources.

The wet deposition patterns of the mercury species are mainly determined by the precipitation patterns. Hg^2 is also highly soluble so it dominates the wet deposition pattern of gaseous mercury. Therefore the maximum wet deposition of Hg^2 is calculated during major precipitation events and at those positions where mercury emissions are high. The wet deposition pattern of Hg^2 is illustrated in Figure 4c. Figure 4d illustrates the wet deposition of Hg^P after 10 days of simulation. It is evident that over the mountainous areas, where the total amount of precipitation is higher the wet deposition of the particulate mercury is larger. Inspection of Figures 4c, d indicates that the maximum wet deposition of Hg^2 reaches locally up to 1500 ng/m^2, while for Hg^p it does not exceed 850 ng/m^2. In addition it is evident that Hg^2 wet deposition is almost 30% higher over the New York State than the wet deposition of Hg^P.

The total deposited mercury (wet and dry) for the simulation performed using all available mercury sources was also averaged over the New York State. More specifically, the wet and dry deposition of Hg^P and Hg^2 were calculated using both modelling systems, namely RAMS and SKIRON/Eta. Dry and wet deposition of all mercury species, accumulated for the simulation period and averaged over the entire domain of the State of New York, is shown in Figure 5. Similar behaviour is evident in both models during the simulation period. However, SKIRON/Eta calculated higher amounts of wet and dry deposited mercury. This can be attributed to the precipitation scheme that SKIRON/Eta uses, leading to rainfall events that cover larger areas. Thus the precipitation scheme used by each model can be a controlling factor during calculations of the wet deposition of mercury.

3.3. SIMULATION WITHOUT NY STATE HG EMISSION SOURCES-SCENARIO 2

In the second scenario, simulations were performed without using the sources located in the State of New York. The mercury concentrations calculated in both cases (Scenarios 1 and 2) were then compared. The concentrations of all mercury species (Hg^0, Hg^2, Hg^p) when there are no sources over the State of New York are illustrated in Figures 6a–c respectively and compared with the Figures 3a, b, c.

Minor differences between the Hg^0 concentration patterns appeared mainly downwind the State of New York following the prevailing north-easterly flow during the last days of the simulation period. The differences in both scenarios for Hg^2 concentrations where even up to 100% locally, near the sources locations in the State of New York. This is consistent with the literature as Hg^2 can be removed in the vicinity of a few tens to a few hundreds of kilometres downstream of the source (Figures 3b and 6b). Hg^P concentrations are up to 25% lower within the State of New York compared to the first scenario, not only near the sources locations but also at intermediate from the sources distances (Figures 3c and 6c). The absence

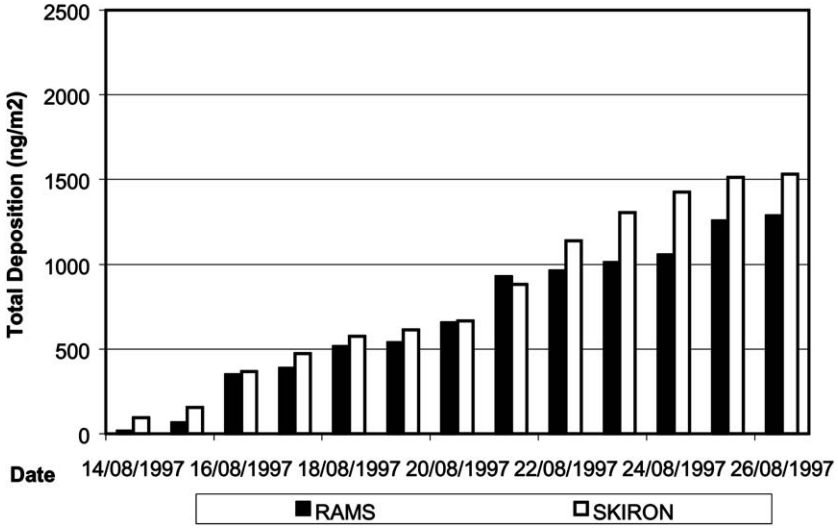

Figure 5. Total deposition of mercury (ng/m^2) calculated from RAMS and SKIRON/Eta systems (with NY State emissions) averaged over NY State from 14 to 26 August 1997.

of emission is likely to exert strong influence not only on the concentration pattern of all species but also on their maximum values.

Wet and dry depositions of all mercury species were also calculated for the second scenario, namely for the simulation performed without using the sources available over the State of New York. When sources of mercury are not considered, the dry and wet deposited amount of all species over the selected area of New York State is lower (see Figures 7a–d). Major differences between the two simulations are evident for Hg^2 and Hg^P since these species are transported in short and intermediate distances respectively.

The two simulations have also been compared for Adirondacks, located in the State of New York. This comparison provided an estimation of the relative contribution of local emissions versus long-range transport to mercury deposition at a specific location. The wet deposition of all mercury species when the New York State sources were not considered reduced up to 15% as illustrated in Figure 8.

The model intercomparison also presented in Figure 8 showed that the wet deposited amounts of mercury calculated using the SKIRON/Eta model were up to 30% higher than those computed by RAMS. The differences appeared between the two models did not exceed 20% in the second scenario (when mercury sources from the State of New York were not used). This could be attributed primarily to differences between the precipitation patterns of both models and the existence/omission of local sources of Hg^2 and Hg^P.

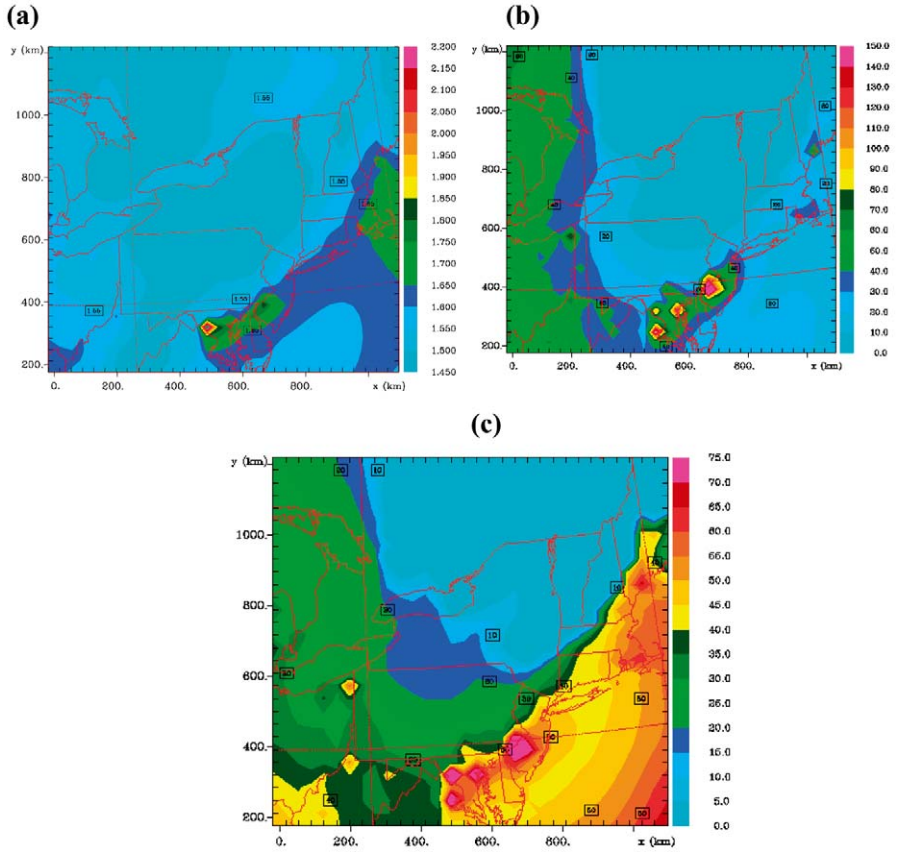

Figure 6. Mercury concentration at the first model level (∼ 69 m) at 0000 UTC on 24 August 1997 from RAMS model (without NY sources) of (a) Hg^0 (in ng/m^3), (b) Hg^2 (in pg/m^3) and (c) Hg^p (in pg/m^3).

4. Observations-Model Calculations Intercomparison

Deposition measurements were available from several locations within the NE part of the US. More specifically, the Mercury Deposition Network (MDN) and the Regional Environmental Monitoring and Assessment Program (REMAP) provided wet deposition measurements at sites upwind and downwind of NY State. A selection of four stations has been made based on the spatial resolution used for the simulation and the consistency of sampling procedures of the measurements.

The selected observations for the MDN stations, namely Allegheny Portage at Pennsylvania, Bridgton and Greenville at Maine represent the weekly measured wet deposition of all mercury species, for the periods 12 to 19 August 1997 and 19 to 26 August 1997. In addition deposition observations performed within the REMAP at Underhill in Vermont, for the periods 13 to 15 August 1997 and 15 to 21 August 1997, have been also utilized. Although the available deposition

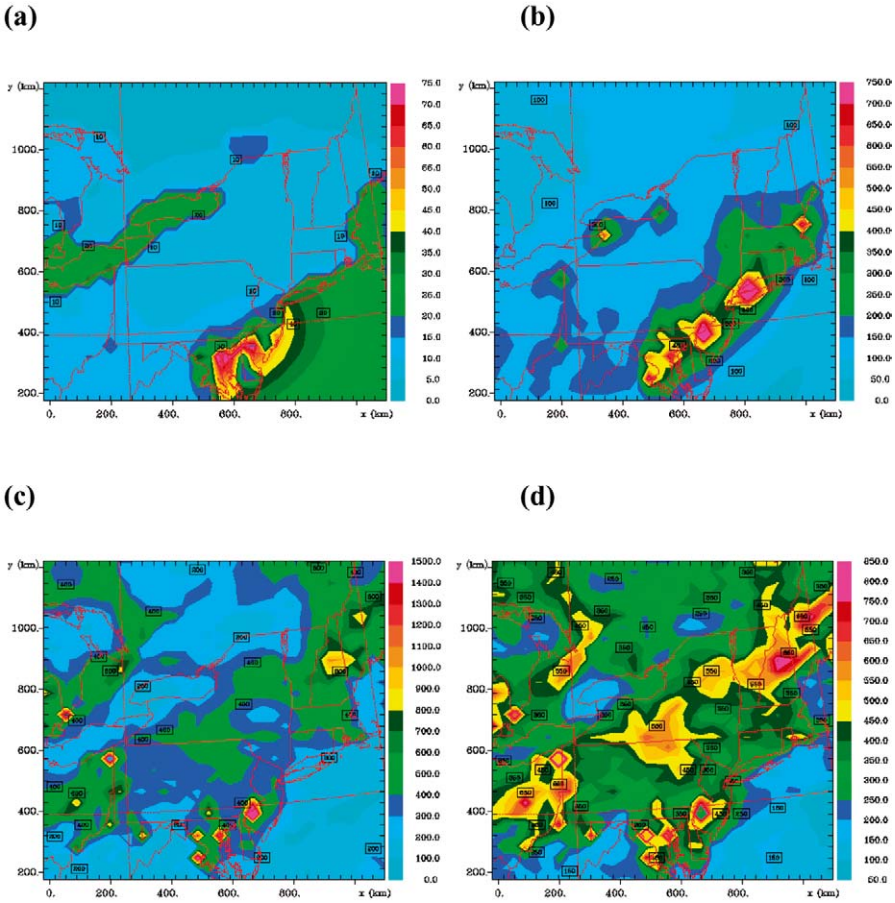

Figure 7. Dry and wet deposition at 0000 UTC on 24 August 1997 after 10 days of simulation, estimated from RAMS model (without NY sources). (a) Dry deposition of Hg^P (in ng/m^2), (b) Dry deposition of Hg^2 (in ng/m^2),(c) Wet deposition of Hg^2 (in ng/m^2) and (d) Wet deposition of Hg^P (in ng/m^2).

observations are limited for the model simulation period, an attempt was made to inter-compare model outputs and observations. Since no information for the starting hour during the sampling periods is available, the observations have been compared with the 0000 UTC model outputs. From the model outputs accumulated wet deposition of all mercury species have been calculated for all 12 days of simulation. The wet deposition values of the mercury species have been accumulated from the initial time of the simulation, for both scenarios for the entire simulation period. A similar accumulation has also been made for the observations, in order to achieve greater consistency between the observations and model calculations.

The inter-comparison between model calculations and observations was made with both models, for both scenarios and the results are illustrated in Figures 9a–d. Both models tend to overestimate the deposited amounts of mercury species

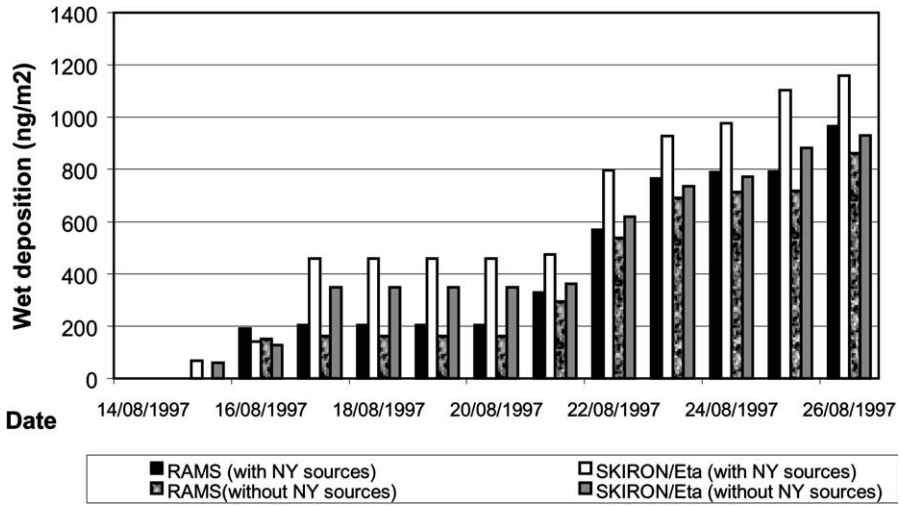

Figure 8. Comparison of the accumulated wet deposition of mercury (ng/m^2) calculated from RAMS and SKIRON/Eta models (without NY State emissions) at Adirondacks from 14 to 24 August 1997.

at about 20–30%. However these overestimated deposited quantities of mercury, from both models, can be considered within the acceptable limits by taken into account uncertainties in measuring both emissions and depositions. Several factors, such as observational errors, uncertainties of the observation network, weekly type measurements, as well as differences on the precipitation scheme of both models should be considered. It is well known that the spatial distribution of precipitation is affected by the large scale rain and convective parameterisation [28]. It is also worth mentioning that even a small shift (temporal or spatial) in the model estimated rain pattern during the observation period, can strongly influence the model deposition values.

When the NY State local emissions were not used during the simulation period, the accumulated wet deposition is (as expected) lower. Thus the reduction of the Hg^2 and Hg^P emissions, considered as meso-β and meso-a scale transport pollutants respectively, over specific locations can reduce the deposited amounts of mercury over the region and consequently minimize its effects on human population.

5. Conclusions

This study was focused on estimating the in/out of state contribution of mercury sources to the total deposited mercury over the State of New York. This was achieved by utilizing two well-known atmospheric modelling systems with modules describing the atmospheric mercury processes incorporated. Two different scenarios have been investigated. The comparison of both scenarios showed that

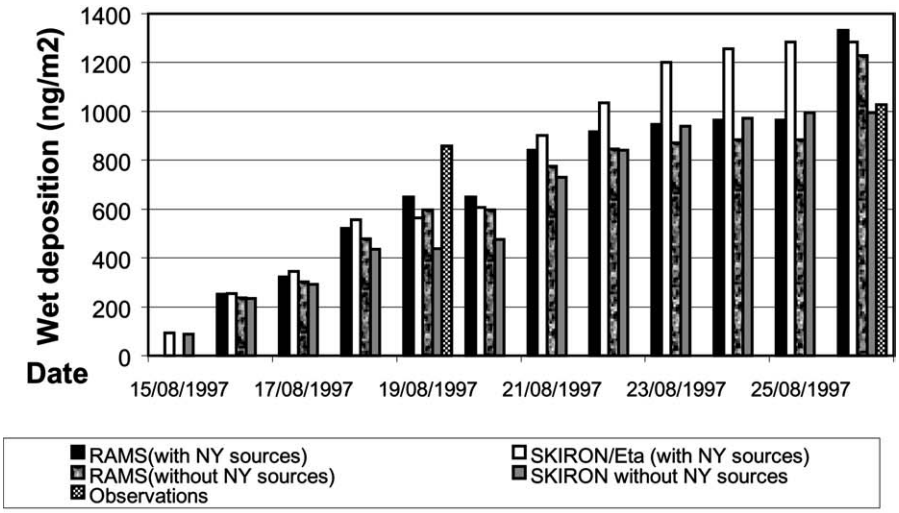

(a)

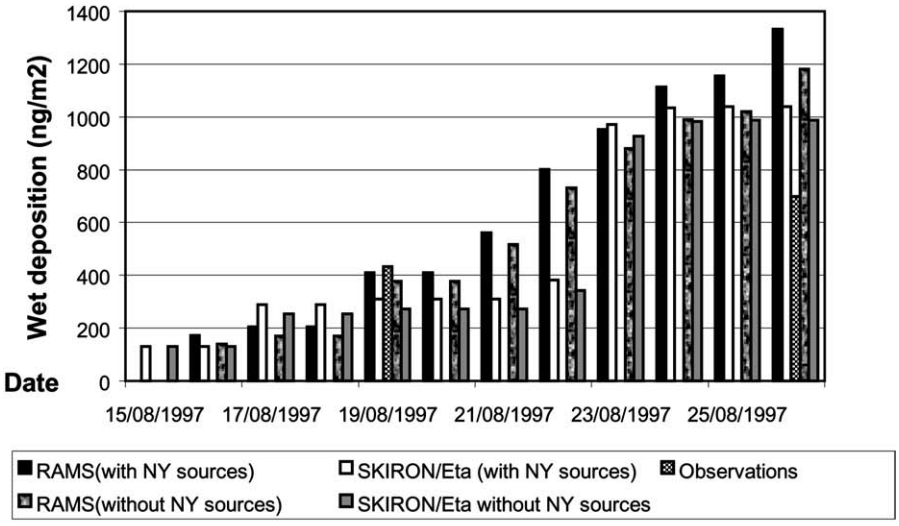

(b)

Figure 9. Comparison of observations of wet deposition of mercury (ng/m^2), RAMS and SKIRON/Eta outputs (both scenarios) from 15 to 26 August 1997. RAMS and SKIRON/Eta outputs are accumulated since the initial time of the simulation, while the observations correspond to weekly-deposited mercury at (a) Allegheny, (b) Bridgton (c) Greenville and (d) Underhill.

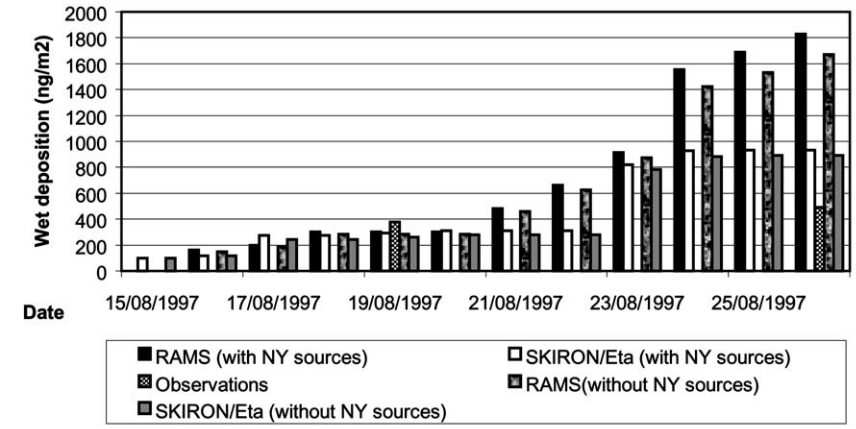

(c)

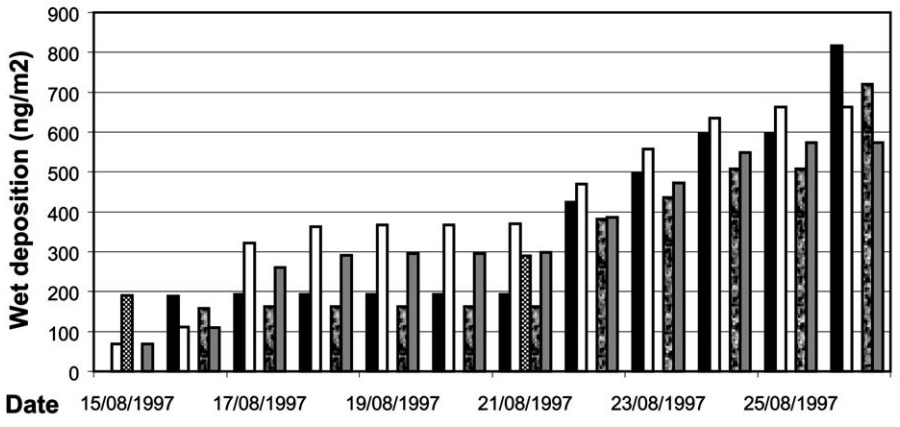

(d)

Figure 9. Continued.

Hg^2 and Hg^P concentrations, as well as the prevailing meteorological conditions (mainly precipitation and turbulence) affect the deposited amounts of mercury over a specific area. Hg^2 and Hg^P are known to be local and regional scale pollutants, respectively. Thus reduction of mercury emissions from anthropogenic sources regionally, could lead to the progressive amelioration of the atmospheric mercury problem.

Given the limited number of the available observations of the wet deposition of mercury the results obtained from the comparison with the model outputs are

encouraging. Major problems have been avoided because the mercury modules are coupled to the atmospheric models on a direct way. The coupling of mercury processes with the atmospheric model is useful on avoiding limitations derived by the use of rather simplified chemical mechanisms. However, a systematic model evaluation is difficult unless some other controlling factors, such as more accurate emission inventories and detailed (quality/quantity) observations are available. Wet deposition observations must be available, at least on a daily basis, to compare against model results of longer simulation periods.

The difficulties in measuring the wet and dry deposition of mercury make the deposition patterns estimated by the model very useful. Thus, a well-developed numerical model is much cheaper to run than a dense observation network that is required for high-resolution estimations of the concentration and deposition. From this aspect the developed models should be considered as useful tools for studying the mercury processes and therefore useful in accessing various emission control strategies.

Acknowledgements

The authors wish to acknowledge New York State Energy Research and Development Authority (NYSERDA #6488) for funding within the framework of Atmospheric Transport and Fate of Mercury and its Impact on New York State project (SUBAWARD# 01-9RF PTAEO#1015266-20439-1). The main model development was performed during MAMCS project (ENV4-CT97-0593) while the present work was partially supported by ADIOS (EVK3-CT-2000-00035) and MERCYMS (EVK3-2002-00070) projects of the DG-Research of EU. The two anonymous reviewers are also acknowledged.

References

1. Walko, R.L. and Tremback, C.J.: 1996, *RAMS – The Regional Atmospheric Modelling System* Version 3b: *User's Guide*, ASTeR, Inc., P.O. Box 466, Fort Collins, Colorado, 86 pp.
2. Pielke, R.A., Cotton W.R., Walko R.L., Tremback C.J., Lyons W.A., Grasso L.D., Nicholls M E., Moran M.D., Wesley D.A., Lee T.J. and Copeland, J.H.: 1992, A Comprehensive Meteorological Modelling System – RAMS, *Meteorol. Atmos. Phys.* **49**, 69–91.
3. Kallos, G., Nickovic, S., Papadopoulos, A., Jovic, D., Kakaliagou, O., Misirlis, N., Boukas, L., Mimikou, N., Sakellaridis, G., Papageorgiou, J., Anadranistakis, E. and Manousakis, M.: 1997, The Regional Weather Forecasting System SKIRON. In: *Proceedings of the Symposium on Regional Weather Prediction on Parallel Computer Environments*, 15–17 October 1997, Athens, Greece, pp. 109–122.
4. Papadopoulos, A., Katsafados, P., Kallos, G. and Nickovic, S.: 2002, 'The Poseidon Weather Forecasting System: An Overview', *Glob. Atmos. Ocean Syst.* **8**, 219–237.
5. Lindqvist, O., Johansson, K., Aastrup, M., Andersson, A., Bringmark, L., Hovsenius, G., Hakanson, Iverfeldt, A., Meili, M. and Timm, B.: 1991, Mercury in the Swedish Environment – Recent Research on Causes, Consequences and Corrective Methods, *Water Air Soil Pollut.* **55**, 1–26.

6. Jackson, T.A.: 1997, Long-Range Atmospheric Transport of Mercury to Ecosystems, and the importance of Anthropogenic Emissions – A Critical Review and Evaluation of the Published Evidence, *Environ. Rev.* **5**, 99–120.
7. Xu, X., Yang, X., Miller, D.R., Helble, J.J. and Carley R.J.: 1999, Formulation of Bi-Directional Atmosphere-Surface Exchanges of Elemental Mercury, *Atmos. Environ.* **33** 4345–4355.
8. Vandal, G.M., Fitzgerald, W.F., Lamborg C.H. and Rolfjus K.R.: 1993, The Production and Evasion of Elemental Mercury in Lakes: A Study of Pallette Lake, Northern Wisconsin, U.S.A. In: *Proceedings of 9th International Conference on Heavy Metals in the Environment*, pp. 297–300, CEP Consultants Ltd., Heavy Metals Secreatariat, Edinburgh, U.K.
9. Fitzgerald, W.F., Engstrom, D.R., Mason, R.P. and Nater, E.A.: 1997, The Case for Atmospheric Mercury Contamination in remote areas, *Environ. Sci. Tech.* **32**, 1–7.
10. Ariya, P.A., Khalizov, A. and Gidas, A.: 2002, Reactions of gaseous mercury with Atomic Molecular Halogens: Kinetics, Product Studies, and Atmospheric Implications, *J. Phys. Chem.* A 2002, **106**, 7310–7320.
11. Pirrone, N., Hedgecock, I.M. and Forlano L.: 2000, Role of the Ambient Aerosol in the Atmospheric Processing of Semi-Volatile Contaminants: A Parameterized Numerical Model (GASPAR), *J. Geophys. Res.* **105**, 9773–9790.
12. Gershenzon, M., Davidovits, P., Jayne, J.T., Kolb, C.E. and Worsnop, D.R.: 2002, Rate Constant for the Reaction of Cl_2(aq) with OH^-, *J. Phys. Chem.* A 2002, **106**, 7748–7754.
13. Williams, R.M.: 1982, A Model for the Dry Deposition of Particles to Natural Water Surfaces, *Atmos. Environ.* 1933–1938.
14. Pirrone, N., Keeler G.J. and Holsen, T.M.: 1995a, Dry Deposition of Trace Elements over Lake Michigan: A Hybrid-Receptor Deposition Modelling Approach, *Environ. Sci. Technol.*, **29**, 2112–2122.
15. Pirrone, N., Glinsorn G. and Keeler, G.J.: 1995b, Ambient Levels and Dry Deposition Fluxes of Mercury to Lakes Huron, Erie and St. Clair, *Water Air Soil Pollut.* **80**, 179–188.
16. Slinn, S.A. and Slinn, W.G.N.: 1981, Modelling of Atmospheric Particulate Deposition to Natural Waters. In: *Atmospheric Pollutants in Natural Waters*, S.J. Eisenreich (ed.), Ann Arbor Science, Ann Arbor, MI, pp. 22–53.
17. Hicks, B.B., Baldocchi D.D., Hosker R.P. Jr., Hutchison B.A., Matt D.R., McMillen R.T. and Satterfield, L.C.: 1985, *On the Use of Monitored Air Concentrations to Infer Dry Deposition*. NOAA Technical Memorandum ERL ARL-141, Silver Spring, MD.
18. Pai, P., Karamchandani, P. and Seigneur, C.: 1997, Simulation of the Regional Atmospheric Transport and Fate of Mercury Using a Comprehensive Eulerian Model, *Atmos. Environ.* **31**, 2717–2732.
19. Walcek, C., De Santis, S., Gentile, T.: 2003, Preparation of Mercury Emissions Inventory for Eastern North America, *Environ. Pollut.* **123**, 375–381.
20. Slemr F., Junkermann, W., Schmidt, R.W..H. and Sladkovic, R.: 1995, Indication of Change in Global and Regional Trends of Atmospheric Mercury Concentrations, *GRL* **22**, 2143–2146.
21. Electric Power Research Institute Technical Report TR-107695, 1996: *Mercury in the Environment – A Research Update*, Final report, EPRI, Palo Alto, CA.
22. Xu, X., Yang, X., Miller, D.R., Helble, J.J., Thomas H. and Carley R.J.: 2000, A Sensitivity Analysis on the Atmospheric Transformation and Deposition of Mercury in North-Eastern USA, *Sci. Total Environ.* **259**, 169–181.
23. Shannon, J.D. and Voldner, E.C.: 1995, Modelling atmospheric Concentrations of Mercury and Deposition to the Great Lakes, *Atmos. Environ.* **29**, 1649–1661.
24. Murphy D.M., Thompson, D.S. and Mahoney, M.J.: 1998, *In Situ* Measurements of Organics, Meteoritic Material, Mercury, and Other Elements in Aerosols at 5 to 19 kilometers, *Science* **282**, 1664–1669.
25. Betts, A.K.: 1986, A New Convective Adjustment Scheme. Part E. Observational and Theoretical Basis, *Quart. J. R. Met. Soc.* **112**, 677–691.

26. Davies, F. and Notcutt, G.: 1996, Biomonitoring of Atmospheric Mercury in the Vicinity of Kilauea, Hawaii, *Water Air Soil Pollut.* **86**, 275–281.
27. Schroeder, W. and Munthe, J.: 1998, Atmospheric Mercury – An Overview, *Atmos. Environ.* **32**, 809–822.
28. Colle, B.A., Mass, C. and Westrick, K.J.: 2000, MM5 Precipitation Verification over the Pacific Northwest during the 1997–99 Cool Seasons,. *Wea. Forecast.* **15**, 730–745.
29. Clever H.L, Johnson S.A. and Derrick, M.E.: 1985, The Solubility of Mercury and Some Sparingly Soluble Mercury Salts in Water and Aqueous Electrolyte Solutions, *J. Phys. Chem.* Ref. Data **14**, 632–680.
30. Lin, C. and Pehkonen, S.O.: 1997, Aqueous Free Radical Chemistry of Mercury in the Presence of Iron Oxides and Ambient Aerosol, *Atmos. Environ.* **31**, 4125–4137.
31. Lin, C. and Pehkonen, S.O.: 1998, Two-Phase Model of Mercury Chemistry in the Atmosphere, *Atmos. Environ.* **32**, 2543–2558.
32. Mediterranean Atmospheric Mercury Cycle System (MAMCS): 2000, *ENV4-CT97-0593*, Technical Report, 264 p.
33. Munthe, J., Xiao, Z.F. and Lindqvist, O.: 1991, The Aqueous Reduction of Divalent Mercury by Sulfite, *Water Air Soil Pollut.* **56**, 621–630.
34. Munthe, J.: 1992, The Aqueous Oxidation of Elemental Mercury by Ozone, *Atmos. Environ. Part A-Gen. Topics* **26**, 1461–1468.
35. Pehkonen, S.O. and Lin, C.: 1998, Aqueous Photochemistry of Mercury with Organic Acids, *J. Air Waste Manage. Assoc.* **48**, 144–150.
36. Pleijel, K. and Munthe, J.: 1995, Modelling the Atmospheric Chemistry of Mercury – The Importance of a Detailed Description of the Chemistry of Cloud Water, *Water Air Soil Pollut.* **80**, 317–324.
37. Walko, R.L., Cotton, W.R., Meyers, M.P. and Harrington, J.Y.: 1995, New RAMS Cloud Microphysics Parameterization, Part I: The Single Moment Scheme, *Atmos. Res.* **38**, 29–62.
38. Wesely M.L. and Hicks, B.B.: 2000, Review on the Current Status of Knowledge on Dry Deposition, *Atmos. Environ.* **34**, 2261–2282.